OPEN ACCESS
CellPress

Cell Reports
Report

Free Radicals Mediate Systemic Acquired Resistance

Caixia Wang,[1,2] Mohamed El-Shetehy,[2] M.B. Shine,[2] Keshun Yu,[2] Duroy Navarre,[3] David Wendehenne,[4] Aardra Kachroo,[2] and Pradeep Kachroo[2,*]
[1]College of Agronomy and Plant Protection, Qingdao Agricultural University, Qingdao 266109, P.R. China
[2]Department of Plant Pathology, University of Kentucky, Lexington, KY 40546, USA
[3]U.S. Department of Agriculture - Agricultural Research Service, Washington State University, Prosser, WA 99350, USA
[4]Université de Bourgogne, ERL CNRS 6300, UMR 1347 Agroécologie, BP 86510, 21065 Dijon, France
*Correspondence: pk62@uky.edu
http://dx.doi.org/10.1016/j.celrep.2014.03.032

SUMMARY

Systemic acquired resistance (SAR) is a form of resistance that protects plants against a broad spectrum of secondary infections. However, exploiting SAR for the protection of agriculturally important plants warrants a thorough investigation of the mutual interrelationships among the various signals that mediate SAR. Here, we show that nitric oxide (NO) and reactive oxygen species (ROS) serve as inducers of SAR in a concentration-dependent manner. Thus, genetic mutations that either inhibit NO/ROS production or increase NO accumulation (e.g., a mutation in S-nitrosoglutathione reductase [GSNOR]) abrogate SAR. Different ROS function additively to generate the fatty-acid-derived azelaic acid (AzA), which in turn induces production of the SAR inducer glycerol-3-phosphate (G3P). Notably, this NO/ROS→AzA→G3P-induced signaling functions in parallel with salicylic acid-derived signaling. We propose that the parallel operation of NO/ROS and SA pathways facilitates coordinated regulation in order to ensure optimal induction of SAR.

INTRODUCTION

Cell-to-cell communication and long-distance signaling play a key role in the induction of broad-spectrum disease resistance in plants, commonly known as systemic acquired resistance (SAR). SAR involves the generation of a signal (or signals) in the primary leaves that upon translocation to the distal tissues activates defense responses resulting in broad-spectrum resistance. Production of this phloem-based mobile signal occurs within 6 hr of pathogen infection in the primary leaves (Chanda et al., 2011), and the signal is rapidly transferred to the distal uninfected tissues (Kachroo and Robin, 2013).

Several chemicals that contribute to SAR have been identified (reviewed in Shah and Zeier, 2013; Kachroo and Robin, 2013; Gao et al., 2014), including the phytohormone salicylic acid (SA), its methylated derivative MeSA, the dicarboxylic acid azelaic acid (AzA), and the phosphorylated sugar glycerol-3-phosphate (G3P). In addition, SAR is also dependent on the lipid-transfer-like proteins (LTPs) Defective in Induced Resistance (DIR1) (Maldonado et al., 2002; Chanda et al., 2011; Champigny et al., 2011; Yu et al., 2013) and AzA insensitive (AZI1) (Jung et al., 2009), as well as physical factors such as the plant cuticle (Xia et al., 2009, 2010, 2012). In contrast to SA, MeSA, and G3P, genetic evidence supporting the absolute requirement for AzA biosynthesis in SAR remains lacking. AzA is derived from the hydrolysis of 18 carbon (C) fatty acids (FAs) containing a double bond at C9 (Zoeller et al., 2012; Yu et al., 2013). Thus, oleic (18:1), linoleic (18:2), and linolenic (18:3) acids all serve as precursors for AzA. This precursor redundancy and the dependence of plant health on precursor FAs complicate efforts to test the absolute requirement for AzA in SAR.

The diverse chemical nature of SAR-inducing chemicals has led to a growing belief that SAR might involve an interplay among multiple diverse and independent signals (Dempsey and Klessig, 2012). Since metabolic networks often operate as branched pathways, these chemical signals are likely to participate in one or more signaling cascades that eventually merge to induce SAR. Indeed, recent findings that AzA acts upstream of G3P suggest that SAR involves synchronized signaling from diverse signaling chemicals (Yu et al., 2013). However, the relationship between AzA/G3P and SA, which is thought to act at a downstream step in the SAR pathway, remains unknown. Here, we show that SA acts in parallel with two chemical signals, nitric oxide (NO) and reactive oxygen species (ROS), and the simultaneous activation of both SA- and NO/ROS-mediated pathways is essential for the normal induction of SAR. We further show that NO/ROS act upstream of AzA/G3P, and ROS-mediated chemical cleavage of FAs plays an important role in the induction of SAR. Our data elucidate the interrelationships among these diverse chemicals and provide a possible mechanism for the coordinated induction of SAR.

RESULTS AND DISCUSSION

Exogenous Application of an NO Donor Confers SAR

Basal SA is essential for AzA- and G3P-mediated SAR (Jung et al., 2009; Chanda et al., 2011; Yu et al., 2013), whereas NO is known to function upstream of SA (Durner et al., 1998). Furthermore, 18:1 FA, which can serve as a precursor for AzA and thereby induce G3P biosynthesis, also regulates NO levels via its association with the NO Associated 1 (NOA1) protein (Mandal et al., 2012). This suggests a possible link between NO- and

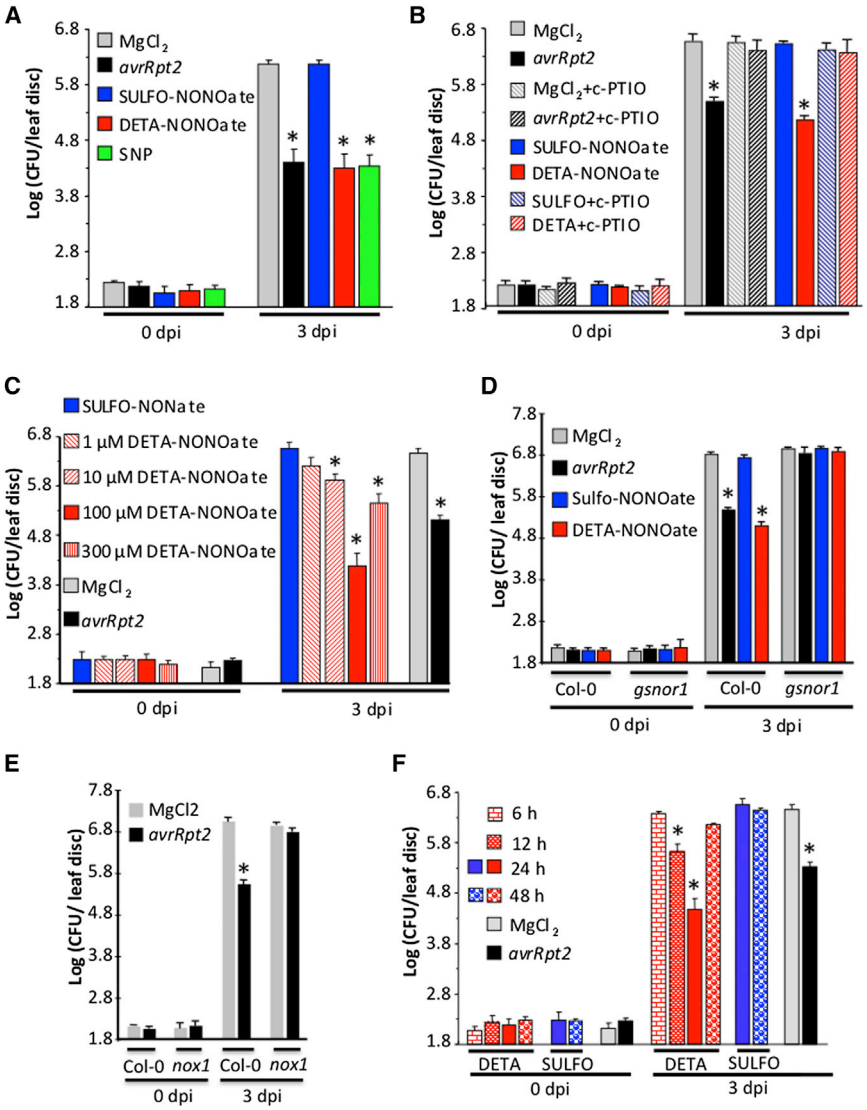

Figure 1. NO Confers SAR in a Dose-Dependent Manner

(A) SAR response in distal leaves of WT Col-0 plants treated locally with $MgCl_2$, avirulent pathogen (*avrRpt2*), SULFO-NONOate, DETA-NONOate, or SNP (100 μM each). The virulent pathogen (DC3000) was inoculated 24 hr after local treatments. Error bars indicate SD (n = 4).

(B) SAR response in distal leaves of WT Col-0 plants treated locally with $MgCl_2$, avirulent pathogen (*avrRpt2*), SULFO-NONOate, or DETA-NONOate (100 μM each), with or without c-PTIO (500 μM). The virulent pathogen (DC3000) was inoculated 24 hr after local treatments. Error bars indicate SD (n = 4).

(C) SAR response in distal leaves of WT Col-0 plants treated locally with $MgCl_2$, avirulent pathogen (*avrRpt2*), SULFO-NONOate (100 μM each) and different concentrations of DETA-NONOate (1–300 μM). The virulent pathogen (DC3000) was inoculated 24 hr after local treatments. Error bars indicate SD (n = 4).

(D) SAR response in distal leaves of Col-0 and *gsnor1* plants treated locally with $MgCl_2$, avirulent pathogen (*avrRpt2*), SULFO-NONOate, or DETA-NONOate (100 μM each). The virulent pathogen (DC3000) was inoculated 24 hr after local treatments. Error bars indicate SD (n = 4).

(E) SAR response in distal leaves of Col-0 and *nox1* plants treated locally with $MgCl_2$ or avirulent pathogen (*avrRpt2*). The virulent pathogen (DC3000) was inoculated 24 hr after local treatments. Error bars indicate SD (n = 4).

(F) SAR response in distal leaves of Col-0 plants treated locally with $MgCl_2$, avirulent pathogen (*avrRpt2*), SULFO-NONOate, or DETA-NONOate (100 μM each). The virulent pathogen (DC3000) was inoculated at the indicated hours after local treatments. Error bars indicate SD (n = 4).

Asterisks denote significant differences with mock-treated plants (t test, $p < 0.05$) and results are representative of three independent experiments. See also Figure S1.

FA→AzA→G3P-mediated SAR. We investigated such a connection by analyzing NOA1 levels in pathogen-infected plants. Interestingly, the NOA1 protein accumulated in both local and distal tissues in response to infection by *Pseudomonas syringae* pv *tomato* (*Pst*) (Figure S1A). Furthermore, NOA1 levels in distal tissues were consistently higher than those in infected leaves. Then, a time-course analysis of NO levels was carried out with the NO-sensitive dye 4-amino-5-methylamino-2,7-difluorofluorescein diacetate (DAF-FM DA; Balcerczyk et al., 2005). Confocal microscopy of *Pst*-infected leaves detected increased DAF-FM DA staining at 6, 12, and 24 hr postinoculation (hpi) (detected as green fluorescence) compared with mock-inoculated plants (Figure S1B), with a maximum increase at 12–24 hpi. A lower but clear increase in NO levels was also detected in the distal (uninoculated) leaves, with peak levels detected at 12 hpi (Figure S1B). The microscopy data correlated well with in vitro fluorescence measurements when the corresponding leaf tissue extracts were incubated with DAF-FM DA (Figure S1C). NO accumulation was further confirmed by performing an alternate assay with a copper-based Cu-FL fluorescent probe, which reacts directly with NO (Lim et al., 2006; Rasul et al., 2012; Figure S1D). We next tested whether the rapidly accumulating NO might serve as a signal for SAR. For this purpose, we preinfiltrated wild-type (WT) plants (ecotype Col-0) with $MgCl_2$, *Pst avrRpt2*, the NO donors 2-(N,N-diethylamino)-diazenolate-2-oxide (DETA-NONOate) and sodium nitroprusside (SNP), or the nitrous oxide donor SULFO-NONOate (negative control). The distal leaves of all plants were then challenged with a virulent strain of *Pst* (DC3000) and the growth of *Pst* DC3000 was monitored at 0 and 3 dpi. WT plants previously infected with *Pst avrRpt2* contained ~10- to 15-fold less *Pst* DC3000 compared with $MgCl_2$ preinfiltrated plants (Figure 1A). Notably, preinfiltration of either DETA-NONOate or SNP, but not SULFO-NONOate, significantly reduced the growth of *Pst* DC3000 (Figure 1A). We then tested the effect of the NO scavenger 2-(4-carboxyphenyl)-4,5-dihydro-4,4,5,5-tetramethyl-1H-imidazolyl-1-oxy-3-oxide (cPTIO) on

this response. Cotreatment with cPTIO abolished both *Pst avrRpt2*- and DETA-NONOate-induced SAR, further reinforcing the importance of NO in SAR (Figure 1B). These results are consistent with the previously proposed role for NO in SAR against tobacco mosaic virus (Song and Goodman, 2001).

Since NO can function in a dose-dependent manner in animal systems (Wink et al., 2011), we tested whether higher or lower doses affected the SAR-inducing ability of NO. SAR was assessed as before in response to preinfiltration of 1–300 μM DETA-NONOate in Col-0 plants. SAR was progressively stronger (as detected by a decrease in *Pst* DC3000 proliferation) in plants infiltrated with increasing concentrations (up to 100 μM) of DETA-NONOate (Figure 1C). Interestingly, however, higher concentrations (300 μM) of DETA-NONOate not only failed to further enhance SAR but also consistently induced significantly weaker SAR. SAR induced by 300 μM DETA-NONOate was comparable to that induced by 10 μM DETA-NONOate. This suggested that NO induced SAR in a concentration-dependent manner. We tested this further by evaluating SAR in genetic mutants (*S*-nitrosoglutathione reductase [*gsnor1*] and NO overproducer [*nox1*]) that constitutively accumulate elevated levels of NO (Figures 1D, 1E, and S1E; He et al., 2004; Blaise et al., 2005). Both mutants were compromised in SAR (Figures 1D and 1E). Moreover, exogenous application of DETA-NONOate failed to induce SAR in the *gsnor1* plants (Figure 1D). This is consistent with the positive regulatory role of *GSNOR1* in plant defense (Feechan et al., 2005). Intriguingly, in contrast to the defective SAR of *gsnor1* plants, antisense downregulation of *GSNOR1* was shown to confer increased disease resistance (Rustérucci et al., 2007). The opposing effects of knockout versus silencing of *GSNOR1* are thought to be due to a partial reduction in GSNOR1 activity in silenced plants as opposed to the complete loss of function in knockout plants (Espunya et al., 2012). This in turn is consistent with the fact that NO confers SAR in a concentration-dependent manner.

To determine the time frame of NO efficacy, we assessed SAR at different times after treatment with 100 μM DETA-NONOate. WT plants were infiltrated with DETA-NONOate; their distal leaves were inoculated with *Pst* DC3000 at 6, 12, 24, or 48 hr after DETA-NONOate infiltration; and *Pst* DC3000 growth was monitored at 0 and 3 dpi. As expected, treatment with SULFO-NONOate was ineffective at inducing SAR or increasing NO levels in the local or distal leaves (Figures 1F, S2A, and S2B). In contrast, pretreatment with DETA-NONOate induced strong SAR and was most effective when applied 24 hr before *Pst* DC3000 infection in the distal leaves, but not after 48 hr (Figure 1F). This correlated well with the time frame of NO accumulation in response to DETA-NONOate treatment in the treated and distal leaves (Figures S2A and S2B). SULFO-NONOate or DETA-NONOate treatment resulted in an insignificant induction of SA-responsive *PR-1* expression in comparison with *Pst avrRpt2* infection (Figure S2C). These data suggest that DETA-NONOate-induced NO likely does not induce SAR by inducing the SA pathway.

noa1 nia1 and *noa1 nia2* Plants Show Compromised SAR

To determine the source of the SAR-inducing NO during pathogen infection, we analyzed SAR in the NO-accumulating and biosynthetic mutants *noa1* and *nia1 nia2*, respectively (Crawford, 2006; Mandal et al., 2012). Notably, the *noa1* and *nia1 nia2* mutants were able to induce SAR, although this SAR was slightly less robust than in WT plants (Figure 2A). Our previous data showed that NO synthesis/accumulation was more significantly compromised in *noa1 nia1* and *noa1 nia2* double mutants, so we analyzed these mutants for SAR (Mandal et al., 2012). Interestingly, and unlike *noa1* or *nia1 nia2*, the *noa1 nia1* and *noa1 nia2* plants were unable to induce SAR (Figure 2A), and this correlated with their inability to accumulate detectable NO in response to pathogen infection (Figures S1D, S2D, and S2E). Together, these results provided crucial genetic evidence supporting the role of NO in SAR. All further analysis was carried out using *noa1 nia2* plants. We next assayed whether the lack of NO affected SAR signal generation or perception. For this purpose, we collected petiole exudates (EX) from WT ($^{Col-0}$EX) and *noa1 nia2* ($^{noa1\ nia2}$EX) plants that were preinfiltrated with either $MgCl_2$ (EX_{MgCl2}) or *Pst avrRpt2* (EX_{AVR}), and infiltrated them into a fresh set of WT and *noa1 nia2* plants (Figure 2B). The distal leaves of all plants were inoculated with *Pst* DC3000 24 hr later, and the growth of *Pst* DC3000 was monitored at 0 and 3 dpi (Figure 2B). $^{noa1\ nia2}EX_{AVR}$ was unable to confer SAR in either WT or *noa1 nia2* plants. In contrast, $^{Col-0}EX_{AVR}$ induced normal SAR in both WT and *noa1 nia2* plants (Figure 2B). Together, these data suggested that the impaired SAR in *noa1 nia2* plants was associated with their inability to generate SAR-inducing signal(s), which in turn was likely due to a defect in pathogen-responsive NO generation.

Since SA is an essential component of SAR and is proposed to function downstream of NO (Durner et al., 1998), we assayed *PR-1* levels in WT and *noa1 nia2* plants in response to $^{Col-0}EX_{AVR}$ and $^{noa1\ nia2}EX_{AVR}$. Both $^{Col-0}EX_{AVR}$ and $^{noa1\ nia2}EX_{AVR}$ induced similar levels of *PR-1* expression in WT and *noa1 nia2* plants (Figure 2C). Although $^{noa1\ nia2}EX_{AVR}$ induced slightly reduced *PR-1* expression in *noa1 nia2* plants, it triggered *PR-1* expression on WT plants similar to that observed for $^{Col-0}EX_{AVR}$. This was consistent with the WT-like SA and SA glucoside levels in the local and distal leaves of pathogen-infected *noa1 nia2* plants (Figure 2D). Together, these results suggested that compromised SAR in *noa1 nia2* plants was not associated with a defect in SA biosynthesis or response.

To assess how SA and NO are related in SAR (if at all), we first tested the possibility of a linear relation (upstream or downstream from each other; see models A and B in Figure S2F). If SA functioned downstream of NO in a linear pathway or in parallel to NO, we expected that exogenous SA would restore SAR in the *noa1 nia2* plants. SA, $MgCl_2$, or *Pst avrRpt2* were infiltrated into WT and *noa1 nia2* plants, followed by *Pst* DC3000 infection in the distal leaves 24 hr later. Monitoring *Pst* DC3000 proliferation at 0 and 3 dpi showed that localized application of SA induced SAR in WT, but not *noa1 nia2*, plants (Figure S3A). Likewise, localized application of the SA derivative MeSA or MeSA+ *Pst avrRpt2* induced SAR in WT, but not *noa1 nia2*, plants (Figure S3B). We next assayed resistance in *noa1 nia2* plants after whole-plant treatment with SA. Whole-plant application of SA only slightly enhanced resistance to *Pst* DC3000 (Figure S3C), suggesting that the *noa1 nia2* plants might be insensitive to SA. However, the SA-treated *noa1 nia2* plants were able to

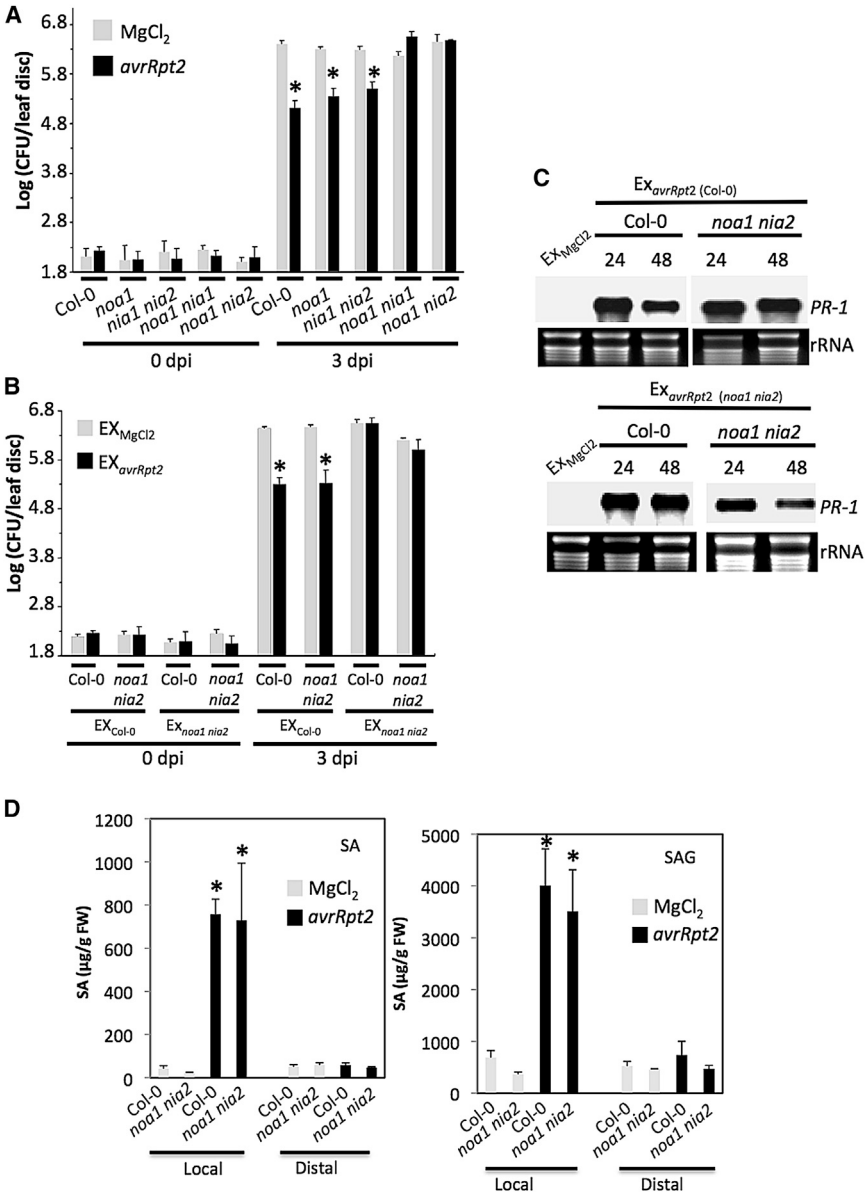

Figure 2. NO Biosynthesis Mutants Show Comprised SAR but Accumulate Normal SA Levels

(A) SAR response in distal leaves of Col-0 and indicated mutants treated locally with $MgCl_2$ or avirulent pathogen (*avrRpt2*). The virulent pathogen (DC3000) was inoculated 48 hr after local treatments. Error bars indicate SD (n = 4).

(B) SAR response in Col-0 and *noa1 nia2* plants infiltrated with petiole exudates collected from Col-0 or *noa1 nia2* plants that were treated either with $MgCl_2$ (EX_{MgCl2}) or *avrRpt2* ($EX_{avrRpt2}$). The distal leaves were inoculated with virulent pathogen at 48 hr after infiltration of primary leaves. Error bars indicate SD (n = 4).

(C) RNA gel blot showing transcript levels of *PR-1* in Col-0 and *noa1 nia2* leaves infiltrated with petiole exudates collected from Col-0 (upper panel) or *noa1 nia2* (lower panel) plants that were treated either with $MgCl_2$ (EX_{MgCl2}, first lane) or *avrRpt2* ($EX_{avrRpt2}$, second lane). Leaves were sampled 24 or 48 hr after treatments. Ethidium bromide staining of rRNA was used as loading control.

(D) SA (left panel) and SAG (right panel) levels in mock- ($MgCl_2$) or avirulent pathogen-inoculated (*avrRpt2*) local and distal leaves of Col-0 and *noa1 nia2* plants 48 hr after inoculation.

In (A), (B), and (D), asterisks denote significant differences compared with ethanol-treated plants (t test, $p < 0.05$). Results are representative of two (C and D) or three (A and B) independent experiments. Error bars indicate SD (n = 4). See also Figure S2.

induce similar levels of *PR-1* expression as WT plants, indicating otherwise (Figure S3D). Together, these results suggested that SA does not function downstream of NO in the SAR pathway. We next tested the alternate possibility that NO functions downstream of SA. For this purpose, we tested the ability of DETA-NONOate to induce SAR in mutants defective in accumulation of SA (*sid2* and *eds5*) or MeSA (*bsmt1*), and defective in SA signaling (*npr1* and *pad4*). DETA-NONOate, which induced SAR in WT plants, did not induce SAR in *sid2*, *eds5*, *bsmt1*, *npr1*, or *pad4* (Figure S3E). This ruled out the possibility that NO functions downstream of SA. Together, these results suggest that NO and SA confer SAR via independent pathways (model C in Figure S2F). This model is further strengthened by the fact that plants cotreated with both SA and DETA-NONOate showed stronger SAR (Figure S3F), and that *sid2* and *noa1 nia2* mutants accumulated normal levels of NO and SA (Figures 2D, S1D, and S3G), respectively.

ROS Is Required for SAR and Operates in a Feedback Loop with NO

Since NO is intricately connected to ROS (Scheler et al., 2013), we next assessed whether ROS induced SAR. WT plants were preinfiltrated with water or H_2O_2, the distal leaves of all plants were challenged with *Pst* DC3000, and bacterial growth was monitored at 0 and 3 dpi. Plants preinfiltrated with H_2O_2, but not water, showed significantly reduced bacterial growth, and this was comparable to the growth of *Pst* DC3000 in plants preinfected with *Pst avrRpt2* (Figure 3A). This suggested that, like NO, H_2O_2 was a potent inducer of SAR in WT plants. To determine the dose-response relationship, we assayed SAR following localized preinfiltration of 5–1,500 µM H_2O_2 in WT plants. As with NO, preinfiltration of lower concentrations of H_2O_2 (5–500 µM) induced progressively stronger SAR, whereas a higher concentration (1.5 mM) was less effective (Figure 3A). This suggested that, as with NO, H_2O_2-triggered SAR was concentration dependent. To determine the time frame of H_2O_2 efficacy, SAR was assessed at different times (6, 12, 24, or 48 h)

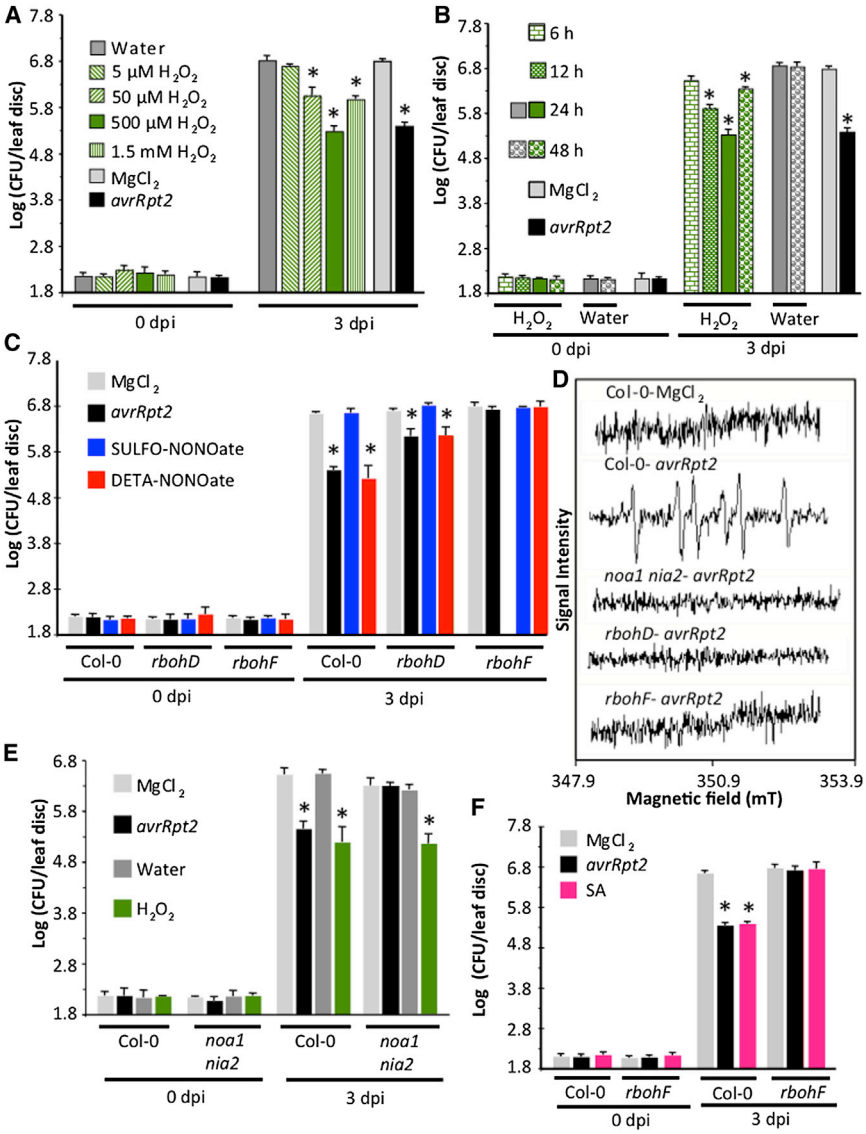

Figure 3. ROS Are Required for SAR in a Dose-Dependent Manner

(A) SAR response in distal leaves of WT Col-0 plants treated locally with $MgCl_2$, avirulent pathogen (*avrRpt2*), and different concentrations of H_2O_2. The virulent pathogen (DC3000) was inoculated 24 hr after local treatments.

(B) SAR response in distal leaves of Col-0 plants treated locally with $MgCl_2$, avirulent pathogen (*avrRpt2*), or H_2O_2 (500 μM each). The virulent pathogen (DC3000) was inoculated at the indicated hours after local treatments.

(C) SAR response in distal leaves of Col-0 and *rboh* mutants treated locally with $MgCl_2$, avirulent pathogen (*avrRpt2*), SULFO-NONOate, or DETA-NONOate (100 μM each). The virulent pathogen (DC3000) was inoculated 24 hr after local treatments.

(D) ESRS spectra showing superoxide anion radical levels in distal leaves of mock- and *avrRpt2*-inoculated Col-0, *rboh*, and *noa1 nia2* plants. The leaves were sampled at 24 hpi and EMPO was used as the spin trap.

(E) SAR response in distal leaves of Col-0 and *noa1 nia2* plants treated locally with $MgCl_2$, avirulent pathogen (*avrRpt2*), or H_2O_2 (500 μM each). The virulent pathogen (DC3000) was inoculated 24 hr after local treatments.

(F) SAR response in distal leaves of Col-0 and *rbohF* plants treated locally with $MgCl_2$, avirulent pathogen (*avrRpt2*), or SA (500 μM). The virulent pathogen (DC3000) was inoculated 48 hr after local treatments.

In (A)–(C), (E), and (F), asterisks denote significant differences compared with mock-treated plants (t test, $p < 0.05$). Results are representative of two (D) or three (A–C, E, and F) independent experiments. Error bars indicate SD (n = 4). See also Figure S3.

following localized infiltration of 500 μM H_2O_2. As with NO, H_2O_2-inducible SAR was detected only up to 24 hr after application, with maximum efficacy at 24 hr (Figure 3B). Thus, NO and H_2O_2 have common characteristics in terms of dose response and time of efficacy for SAR. This was further supported by a comparison of microarray data sets from NO- and H_2O_2-treated plants: 94 of 148 NO-responsive genes were also upregulated by H_2O_2 (Table S1; Parani et al., 2004). In contrast, only one of the NO-induced genes was induced in response to exogenous SA (At5g34500) and this gene was not induced by H_2O_2 (Table S2).

To test whether the H_2O_2-induced SAR was biologically relevant, we assayed SAR in mutants (respiratory burst oxidase homologs [*rboh*]) defective in ROS production (Torres et al., 2002; Sagi and Fluhr, 2006). The *Arabidopsis* genome encodes ten *RBOH* homologs, but only two of these (*RBOHD* and *RBOHF*) are expressed throughout the plant (Sagi and Fluhr, 2006). Therefore, we tested SAR in these mutants. In the majority of our experiments (four of six), both *rbohF* and *rbohD* were defective in SAR. However, in two of six experiments, *rbohD* showed weak SAR (Figure 3C). Pathogen inoculation induced similar levels of *PR-1* expression in infected and distal tissues of Col-0 and both *rboh* mutants (Figure S3H). Furthermore, the *rboh* mutants were responsive to SA and induced WT-like levels of *PR-1* (Figure S3I). Together, these results suggested that the defective SAR in the *rboh* mutants was not due to a defect in the SA pathway.

We monitored ROS levels in local and distal tissues of the *rboh* mutants to determine whether their compromised SAR correlated with the defect in ROS levels. We used electron spin resonance spectrometry (ESRS) and spectrofluorometry to first quantify free radicals generated in response to mock inoculation and *Pst avrRpt2* infection in WT plants. *Pst avrRpt2* infection induced H_2O_2 accumulation in infected and distal tissues of WT plants at 12 and 24 hpi (Figure S3J). Likewise, ESRS using α-(4-Pyridyl *N*-oxide)-*N*-*tert*-butylnitrone (POBN), which detects hydroxyl- and carbon-centered radicals, revealed increased accumulation of free radicals in local and distal tissues of *Pst*

avrRpt2-infected WT plants (Figure S3K). However, unlike H_2O_2, which accumulated to similar levels in local and distal tissues of WT plants, the highest levels of POBN-trapped free radicals were detected at 12 hpi in local tissues and at 24 hpi in distal tissues (Figure S3K). Quantification of POBN-trapped free radicals in local and distal tissues of *rboh* plants showed significantly reduced levels (Figure S3L), which correlated with their compromised SAR. Similarly, pathogen-inoculated *rboh* mutants did not accumulate superoxide anion radicals, as measured using a 2-ethoxycarbonyl-2-methyl-3,4-dihydro-2*H*-pyrrole-1-oxide (EMPO) spin trap (Figure 3D).

We monitored ROS levels in *noa1 nia2* plants to determine the relationship between NO and ROS during SAR. Interestingly, similar to what was observed for *rboh* mutants, pathogen-infected *noa1 nia2* plants also accumulated reduced levels of H_2O_2, hydroxyl- and carbon-centered radicals, and superoxide anion radicals (Figures 3D, S3J, and S3L). This result suggested that NOA1- and NIA2-derived NO is essential for generating pathogen-inducible ROS, and that ROS likely functions downstream of NO. Consistent with this assumption, localized application of ROS conferred SAR in *noa1 nia2* plants (Figure 3E), whereas DETA-NONOate did not confer SAR on the *rboh* mutants (Figure 3C). Furthermore, localized application of SA was also unable to induce SAR in the *rbohF* plants (Figure 3F). This further supports our hypothesis that NO-ROS and SA comprise two distinct branches of the SAR pathway. We next assayed NO levels in the *rbohF* mutant to determine whether NO and ROS operated in a feedback loop. Interestingly, pathogen infection did not induce detectable NO in *rbohF* plants (Figures S1D and S3M). This suggested that NO and ROS were likely interdependent for accumulation during SAR. This was further supported by the result that localized H_2O_2 application induced the NOA1 protein in both treated and distal tissues (Figure S3N).

ROS Act Additively to Mediate Chemical Hydrolysis of C18 Unsaturated FAs

To obtain further insights into NO/ROS-mediated SAR, we first determined the ability of NO/ROS to confer SAR in mutants defective in the biosynthesis of the SAR inducer G3P or the co-signaling LTPs DIR1 and AZI1 (Yu et al., 2013). Exogenous NO did not induce SAR in the G3P biosynthetic mutant *gli1* (defective in glycerol kinase activity) or the *dir1* and *azi1* mutants (Figure 4A). This suggested that NO/ROS likely function upstream of G3P and DIR1/AZI1. Consistent with this assumption, exogenous G3P was able to confer SAR in *noa1 nia2* and *rbohF* plants (Figure 4B), suggesting a linear connection between NO/ROS and G3P in SAR. Indeed, pathogen infection induced G3P levels in WT, but not *noa1 nia2*, plants (Figure 4C). Since the dicarboxylic acid AzA functions upstream of G3P to induce SAR (Yu et al., 2013), it was possible that reduced G3P levels in *noa1 nia2* plants were associated with a defect in AzA accumulation in the local leaves or its uptake into the distal leaves. We tested this by determining the metabolism and transport of ^{14}C-AzA into local and distal leaves, respectively. Thin-layer chromatography of methylated leaf extracts prepared from ^{14}C-AzA-infiltrated leaves showed a WT-like banding pattern in *noa1 nia2* plants (Figure S4A). Analysis of distal tissues showed that a WT-like fraction of ^{14}C-AzA was transported to distal leaves of *noa1 nia2* plants (Figure S4B). Together, these analyses suggested that the *noa1 nia2* plants were not defective in *in planta* derivatization of AzA in the local leaves or its transport to distal leaves. Similar results were also obtained with the *rboh* mutants (Figures S4A and S4B). Interestingly, unlike the WT, the *noa1 nia2* plants showed only a nominal increase in AzA levels after pathogen infection (Figure 4D), suggesting that their defective SAR was indeed likely associated with their inability to synthesize AzA. This raised the possibility that NO and/or ROS might facilitate the chemical breakage of the C9 double bond in the AzA precursor C18 FAs (Zoeller et al., 2012; Yu et al., 2013). To test this, we assayed the conversion of 18:1, 18:2, or 18:3 FAs to AzA or its intermediate, 9-oxononanoic acid (ONA), using in vitro assays. These FAs were incubated in the presence of DETA-NONOate, H_2O_2, or chemicals that generate superoxide anion radical (photo-oxidation of methylene blue), and singlet oxygen (H_2O_2 + methylene blue) (Mao et al., 1995; Bruchey and Gonzalez-Lima, 2008). The resultant compounds were analyzed by gas chromatography (GC)-mass spectrometry (MS). ROS radicals had varying effects on FAs: superoxide anion radicals were more effective on 18:2 and 18:3 FAs, and singlet oxygen was equally efficient on all C18 FAs (Figure 4E). Exogenous H_2O_2 or DETA-NONOate had no substantial effect on these FAs, but H_2O_2 and $CuSO_4$, which form hydroxyl radicals, increased ONA and AzA levels (Figure 4E). This differential effect of different radicals on FAs suggested that these radicals might act in an additive manner to generate AzA or its precursor ONA. Thus, NO-mediated increased accumulation of ROS serves as one of the early events in SAR establishment, which feeds into the G3P-dependent pathway that operates in parallel with SA to induce SAR. The parallel signaling branches are likely advantageous because they would provide multiple points of regulation, and thus a tighter control of SAR, while also providing opportunities for redundancies in recruiting signaling components. There is in fact precedence for this type of signaling, given the preference for branched pathways in most metabolic networks. For instance, NO has been shown to nitrosylate the central SA signaling component NPR1 (Tada et al., 2008). NO also regulates ROS levels by nitrosylating the RBOHD enzyme (Yun et al., 2011). This might serve as a checkpoint for regulating excessive ROS production, which has a repressive effect on SAR (Figure 4F). However, RBOHF, which plays an equally important role in SAR, is not nitrosylated by NO. This suggests that other mechanisms might also be in place to regulate the activities of various SAR components and/or to coordinate signaling via SA and NO/ROS pathways. Thus, as in the mammalian innate immune response, a fine balance must be maintained between the activation and inhibitory responses associated with plant systemic immunity to allow for the optimal induction of SAR.

EXPERIMENTAL PROCEDURES

Plant Growth Conditions and Pathogen Infections

Plants were grown in MTPS 144 Conviron walk-in chambers at 22°C, 65% relative humidity, and 14 hr photoperiod. The chambers were equipped with cool white fluorescent bulbs (FO96/841/XP/ECO; Sylvania). The photon flux density (PFD) of the day period was 106.9 μmoles m^{-2} s^{-1} (measured using a digital light meter; Phytotronic). Inoculations with *Pseudomonas syringae*

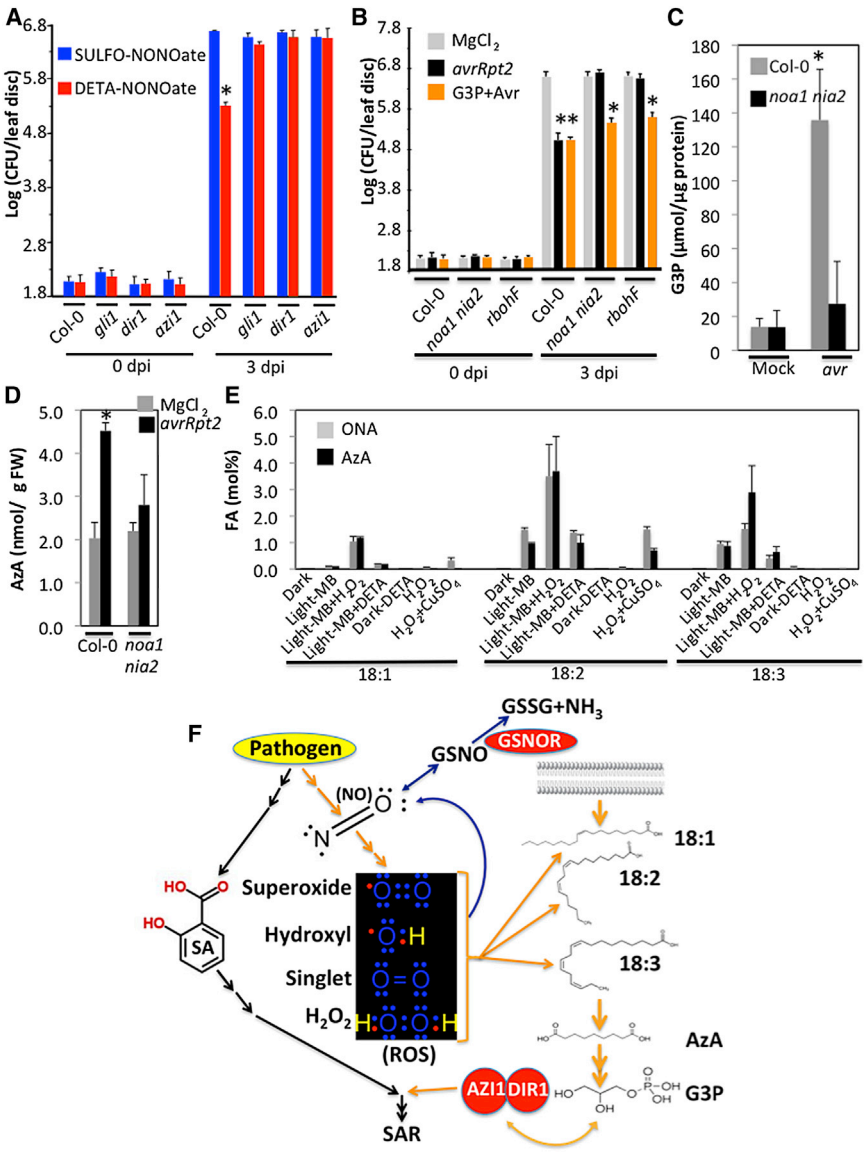

Figure 4. NO and ROS Act Upstream of the AzA-G3P Pathway

(A) SAR response in distal leaves of Col-0 and indicated mutants treated locally with SULFO-NONOate or DETA-NONOate (100 μM each). The virulent pathogen (DC3000) was inoculated 24 hr after local treatments. Error bars indicate SD (n = 4). Asterisks denote significant differences with mock-treated plants (t test, $p < 0.05$) and results are representative of three independent experiments.

(B) SAR response in distal leaves of Col-0, *noa1 nia2*, and *rbohF* plants treated locally with $MgCl_2$, avirulent pathogen (*avrRpt2*), and *avrRpt2* + G3P (100 μM). The virulent pathogen (DC3000) was inoculated 48 hr after local treatments. Error bars indicate SD. Asterisks denote significant differences with mock-treated plants (t test, $p < 0.05$) and results are representative of three independent experiments.

(C) G3P levels in petiole exudates collected from mock- and *avrRpt2*-inoculated Col-0 and *noa1 nia2* plants. Leaves were sampled 24 hr after inoculations. Error bars indicate SD (n = 3). Asterisk denotes significant difference between exudates collected from mock- and *avrRpt2*-inoculated plants (t test, $p < 0.01$). Results are representative of three independent experiments.

(D) AzA levels (per gram fresh weight [FW]) in Col-0 and *noa1 nia2* leaves 24 hr after mock and *avrRpt2* inoculation. Error bars indicate SD (n = 3). Asterisks denote significant differences between mock- and *avrRpt2*-inoculated samples (t test, $p < 0.01$) and results are representative of three independent experiments.

(E) Relative levels of AzA and ONA generated in in vitro reactions where 18:1, 18:2, or 18:3 FAs were incubated in dark or light with methylene blue, H_2O_2, DETA-NONOate, or a combination thereof. To assay the effect of hydroxyl radicals, the FAs were incubated with H_2O_2 + $CuSO_4$.

(F) Simplified model illustrating chemical signaling during SAR. Inoculation of avirulent pathogen triggers independent signaling events that lead to accumulation of SA and NO. NO triggers synthesis of ROS, which act in an additive manner to catalyze oxidation of free C18 unsaturated FAs that are released from membrane lipids (Yu et al., 2013). NO and ROS operate in a feedback loop. Oxidation of C18 FAs generates AzA, which triggers biosynthesis of G3P via upregulation of genes encoding G3P biosynthetic enzymes. G3P and the LTPs DIR1 and AZI1 operate in a feedback loop and depend on each other for their stability. The cellular NO levels are regulated via their storage into GSNO, which can be reduced to glutathione disulfide (GSSG) and NH_3 by GSNOR.
See also Figure S4.

DC 3000 were conducted as previously described (Xia et al., 2009; Chanda et al., 2011). For analysis of SAR, the primary leaves were inoculated with $MgCl_2$ or avirulent bacteria (10^7 cfu ml^{-1}), and 24 hr later the systemic leaves were inoculated with virulent bacteria (10^5 cfu ml^{-1}). Unless noted otherwise, samples from the systemic leaves were harvested at 3 dpi. Petiole exudates were collected as previously described (Chanda et al., 2011).

Detailed experimental procedures are included in the Supplemental Experimental Procedures.

SUPPLEMENTAL INFORMATION

Supplemental Information includes Supplemental Experimental Procedures, four figures, and two tables and can be found with this article online at http://dx.doi.org/10.1016/j.celrep.2014.03.032.

AUTHOR CONTRIBUTIONS

C.W. carried out the bulk of the SAR experiments and NO analysis with help from M.B.S. and M.E.-S. EPR experiments were carried out by M.B.S. with help from M.E.-S. M.E-.S. and C.W. carried out G3P and AzA quantifications. K.Y. carried out TLC analyses. D.N. estimated SA. D.W. helped with NO assays. P.K. and A.K. supervised the project and wrote the manuscript with help from all authors.

ACKNOWLEDGMENTS

This work was supported by grants from the National Science Foundation (MCB-0421914 and IOS-051909) and the United Soybean Board (1244). M.E.-S. was supported by a fellowship from the Egyptian government. We

thank Joanne Holden for help with SA estimations, Guillaume Robin for help with images, Gah-Hyun Lim for help with NO estimations, Evan Stearns for help with expression analysis, Anne-Frances Miller for help with EPR analysis, and Ludmila Lapchyk and Amy Crume for technical support. We thank Nigel Crawford for *noa1*, Dan Klessig for *bsmt1*, Zhen-Ming Pei for *nox1*, Miguel Angel Torres and Jeff Dangl for *rbohD* and *rbohF*, and the Arabidopsis Biological Resource Center for *nia1*, *nia2*, and *gsnor1* seeds.

Received: December 9, 2013
Revised: February 12, 2014
Accepted: March 11, 2014
Published: April 10, 2014

REFERENCES

Balcerczyk, A., Soszynski, M., and Bartosz, G. (2005). On the specificity of 4-amino-5-methylamino-2′,7′-difluorofluorescein as a probe for nitric oxide. Free Radic. Biol. Med. *39*, 327–335.

Blaise, G.A., Gauvin, D., Gangal, M., and Authier, S. (2005). Nitric oxide, cell signaling and cell death. Toxicology *208*, 177–192.

Bruchey, A.K., and Gonzalez-Lima, F. (2008). Behavioral, physiological and biochemical hormetic responses to the autoxidizable dye methylene blue. Am J Pharmacol Toxicol *3*, 72–79.

Champigny, M.J., Shearer, H., Mohammad, A., Haines, K., Neumann, M., Thilmony, R., He, S.Y., Fobert, P., Dengler, N., and Cameron, R.K. (2011). Localization of DIR1 at the tissue, cellular and subcellular levels during Systemic Acquired Resistance in Arabidopsis using DIR1:GUS and DIR1:EGFP reporters. BMC Plant Biol. *11*, 125.

Chanda, B., Xia, Y., Mandal, M.K., Yu, K., Sekine, K.-T., Gao, Q.-M., Selote, D., Hu, Y., Stromberg, A., Navarre, D., et al. (2011). Glycerol-3-phosphate is a critical mobile inducer of systemic immunity in plants. Nat. Genet. *43*, 421–427.

Crawford, N.M. (2006). Mechanisms for nitric oxide synthesis in plants. J. Exp. Bot. *57*, 471–478.

Dempsey, D.A., and Klessig, D.F. (2012). SOS - too many signals for systemic acquired resistance? Trends Plant Sci. *17*, 538–545.

Durner, J., Wendehenne, D., and Klessig, D.F. (1998). Defense gene induction in tobacco by nitric oxide, cyclic GMP, and cyclic ADP-ribose. Proc. Natl. Acad. Sci. USA *95*, 10328–10333.

Espunya, M.C., De Michele, R., Gómez-Cadenas, A., and Martínez, M.C. (2012). S-Nitrosoglutathione is a component of wound- and salicylic acid-induced systemic responses in Arabidopsis thaliana. J. Exp. Bot. *63*, 3219–3227.

Feechan, A., Kwon, E., Yun, B.-W., Wang, Y., Pallas, J.A., and Loake, G.J. (2005). A central role for *S*-nitrosothiols in plant disease resistance. Proc. Natl. Acad. Sci. USA *102*, 8054–8059.

Gao, Q.-M., Kachroo, A., and Kachroo, P. (2014). Chemical inducers of systemic immunity in plants. J. Exp. Bot. http://dx.doi.org/10.1093/jxb/eru010.

He, Y., Tang, R.-H., Hao, Y., Stevens, R.D., Cook, C.W., Ahn, S.M., Jing, L., Yang, Z., Chen, L., Guo, F., et al. (2004). Nitric oxide represses the *Arabidopsis* floral transition. Science *305*, 1968–1971.

Jung, H.W., Tschaplinski, T.J., Wang, L., Glazebrook, J., and Greenberg, J.T. (2009). Priming in systemic plant immunity. Science *324*, 89–91.

Kachroo, A., and Robin, G.P. (2013). Systemic signaling during plant defense. Curr. Opin. Plant Biol. *16*, 527–533.

Lim, M.H., Xu, D., and Lippard, S.J. (2006). Visualization of nitric oxide in living cells by a copper-based fluorescent probe. Nat. Chem. Biol. *2*, 375–380.

Maldonado, A.M., Doerner, P., Dixon, R.A., Lamb, C.J., and Cameron, R.K. (2002). A putative lipid transfer protein involved in systemic resistance signalling in Arabidopsis. Nature *419*, 399–403.

Mandal, M.K., Chandra-Shekara, A.C., Jeong, R.-D., Yu, K., Zhu, S., Chanda, B., Navarre, D., Kachroo, A., and Kachroo, P. (2012). Oleic acid-dependent modulation of NITRIC OXIDE ASSOCIATED1 protein levels regulates nitric oxide-mediated defense signaling in *Arabidopsis*. Plant Cell *24*, 1654–1674.

Mao, Y., Zang, L., and Shi, X. (1995). Singlet oxygen generation in the superoxide reaction. Biochem. Mol. Biol. Int. *36*, 227–232.

Parani, M., Rudrabhatla, S., Myers, R., Weirich, H., Smith, B., Leaman, D.W., and Goldman, S.L. (2004). Microarray analysis of nitric oxide responsive transcripts in Arabidopsis. Plant Biotechnol. J. *2*, 359–366.

Rasul, S., Dubreuil-Maurizi, C., Lamotte, O., Koen, E., Poinssot, B., Alcaraz, G., Wendehenne, D., and Jeandroz, S. (2012). Nitric oxide production mediates oligogalacturonide-triggered immunity and resistance to *Botrytis cinerea* in *Arabidopsis thaliana*. Plant Cell Environ. *35*, 1483–1499.

Rustérucci, C., Espunya, M.C., Díaz, M., Chabannes, M., and Martínez, M.C. (2007). S-nitrosoglutathione reductase affords protection against pathogens in Arabidopsis, both locally and systemically. Plant Physiol. *143*, 1282–1292.

Sagi, M., and Fluhr, R. (2006). Production of reactive oxygen species by plant NADPH oxidases. Plant Physiol. *141*, 336–340.

Scheler, C., Durner, J., and Astier, J. (2013). Nitric oxide and reactive oxygen species in plant biotic interactions. Curr. Opin. Plant Biol. *16*, 534–539.

Shah, J., and Zeier, J. (2013). Long-distance communication and signal amplification in systemic acquired resistance. Front Plant Sci *4*, 30.

Song, F., and Goodman, R.M. (2001). Activity of nitric oxide is dependent on, but is partially required for function of, salicylic acid in the signaling pathway in tobacco systemic acquired resistance. Mol. Plant Microbe Interact. *14*, 1458–1462.

Tada, Y., Spoel, S.H., Pajerowska-Mukhtar, K., Mou, Z., Song, J., Wang, C., Zuo, J., and Dong, X. (2008). Plant immunity requires conformational changes [corrected] of NPR1 via S-nitrosylation and thioredoxins. Science *321*, 952–956.

Torres, M.A., Dangl, J.L., and Jones, J.D.G. (2002). Arabidopsis gp91phox homologues AtrbohD and AtrbohF are required for accumulation of reactive oxygen intermediates in the plant defense response. Proc. Natl. Acad. Sci. USA *99*, 517–522.

Wink, D.A., Hines, H.B., Cheng, R.Y.S., Switzer, C.H., Flores-Santana, W., Vitek, M.P., Ridnour, L.A., and Colton, C.A. (2011). Nitric oxide and redox mechanisms in the immune response. J. Leukoc. Biol. *89*, 873–891.

Xia, Y., Gao, Q.-M., Yu, K., Lapchyk, L., Navarre, D., Hildebrand, D., Kachroo, A., and Kachroo, P. (2009). An intact cuticle in distal tissues is essential for the induction of systemic acquired resistance in plants. Cell Host Microbe *5*, 151–165.

Xia, Y., Yu, K., Navarre, D., Seebold, K., Kachroo, A., and Kachroo, P. (2010). The *glabra1* mutation affects cuticle formation and plant responses to microbes. Plant Physiol. *154*, 833–846.

Xia, Y., Yu, K., Gao, Q.-M., Wilson, E.V., Navarre, D., Kachroo, P., and Kachroo, A. (2012). Acyl CoA Binding Proteins are Required for Cuticle Formation and Plant Responses to Microbes. Front Plant Sci *3*, 224.

Yu, K., Soares, J.M., Mandal, M.K., Wang, C., Chanda, B., Gifford, A.N., Fowler, J.S., Navarre, D., Kachroo, A., and Kachroo, P. (2013). A feedback regulatory loop between G3P and lipid transfer proteins DIR1 and AZI1 mediates azelaic-acid-induced systemic immunity. Cell Rep *3*, 1266–1278.

Yun, B.W., Feechan, A., Yin, M., Saidi, N.B., Le Bihan, T., Yu, M., Moore, J.W., Kang, J.G., Kwon, E., Spoel, S.H., et al. (2011). S-nitrosylation of NADPH oxidase regulates cell death in plant immunity. Nature *478*, 264–268.

Zoeller, M., Stingl, N., Krischke, M., Fekete, A., Waller, F., Berger, S., and Mueller, M.J. (2012). Lipid profiling of the Arabidopsis hypersensitive response reveals specific lipid peroxidation and fragmentation processes: biogenesis of pimelic and azelaic acid. Plant Physiol. *160*, 365–378.